FRAGMENT DETECTION SYSTEM FOR STUDIES OF EXOTIC, NEUTRON-RICH NUCLEI

J.J. Kruse[1], A. Galonsky, C. Snow, E. Tryggestad, J. Wang[2], K. Ieki[a], Y. Iwata[a,3] and P.D. Zecher[4]

We have developed a fragment detection system for use in studies of exotic, neutron-rich nuclei. Using a C-shaped dipole magnet, the system sweeps charged fragments and un-reacted beam particles through an angle before stopping them in an array of plastic scintillator detectors, recording time-of-flight (TOF) and total energy. The system also includes a pair of silicon strip detectors to measure fragment angle of emergence from the target and energy loss for particle identification.

The magnet is a former beam-line dipole magnet from the Bevalac at Berkeley. It is a 7-ton, room temperature, C-shaped magnet with pole faces 33 cm wide x 61 cm long, surrounded by coils 18 cm wide. Neutrons from the target, which is at one end of the magnet (see Fig. 1), have about a 1-m path to the other end. The vertical input to the neutron walls is then determined by the pole gap, which was originally 15 cm. In order to increase the vertical input, an additional 3.8 cm of steel was inserted in the return yoke of the magnet, increasing the vertical gap to 19 cm and the vertical input from 8.7° to 11°. This, of course, reduced the peak magnetic field strength in the gap--from 1.7 T to 1.5 T. We thus made a trade-off of beam deflection angle for event rate. The vertical component of the field was mapped with a hall probe over several horizontal areas of 96.5 cm x 164.6 cm on a grid size of 2.54 cm x 3.05 cm, resulting in 2184 points. With these maps we computed useful fragment trajectories; two are indicated in Fig. 1.

The two Si strip detectors are 250 μm thick, cover an area of 5 cm x 5 cm each, and have sixteen 3-mm-wide horizontal strips which collect free electrons, while the other side has 16 vertical strips which collect electron holes. These strips effectively divide the detector into an array of 2 x 256 (x,y) pixels. The detectors are mounted 15 cm downstream from the target, directly between the coils of the magnet. At a distance of 15 cm from the target, a 3 x 3 mm^2 pixel subtends an angle of 1.15° in each direction.
The signals from the silicon strips are amplified by a set of MSU-constructed S800 pre-amps* and shaped by Washington-University-built, CAMAC controlled shapers [7]. The shaped signals are digitized by Philips peak-sensing ADCs, providing an energy loss measurement as well as x-y pixel information for an angle measurement. In addition to being shaped and digitized, the pre-amp signals are boosted by MSU-built quad fast amplifiers and processed by LeCroy CAMAC constant-fraction discriminators, providing a time signal from the detectors.

The plastic scintillator array stops and measures the total energy of the charged fragments, stops and counts the unreacted beam particles and provides a fast timing signal for neutron velocity measurement. The array is located outside the magnet, 1.7 m downstream from the target location. It consists of 16 vertical bars of fast plastic scintillator, each 4 cm wide, 2 cm thick, and 40.64 cm long. A 2-inch photomultiplier tube (PMT) views each end of each scintillator bar. The 2-cm thickness of the scintillator bars is somewhat greater than the ranges of light fragments with energies of around 30 MeV/A. The horizontal size of the array, 16x4=64 cm, is designed to stop both very rigid unreacted beams such as ^{8}He, as well as fragments such as ^{4}He, which the magnet sweeps through a much larger angle. To minimize scattering of the target neutrons in flight to the Neutron Walls, the exit window from the vacuum chamber is made of a plate of aluminum Hex-Cel honeycomb material. Though it is strong enough to support the atmospheric load of the vacuum, the mass of the 49.5 cm x 66.0 cm window is only 1.36 kg, giving an areal density of 0.4 g/cm^2. Figure 2 shows the scintillator bars and PMTs as they are mounted in the chamber.

---

* Amaxis Systems, Inc., 2817 Olde Gloucester, St. Charles, MO 63301

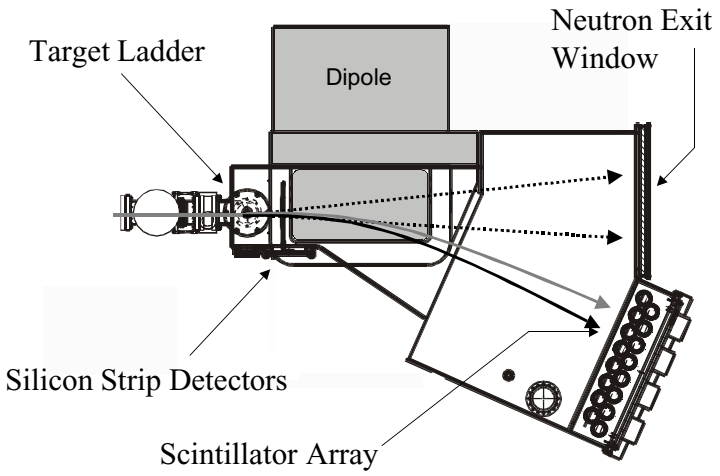

Figure 1 -- Diagram of the Beam Sweeping Dipole, its vacuum chamber, and associated detectors. The beam enters the chamber from the left. Not shown are the position sensitive PPAC detectors, upstream from the target. The grey curve shows the path of an unreacted ^{11}Li particle through the magnet, while the solid black curve shows the path of a ^{9}Li fragment created in the target. The dotted lines represent the paths of two neutrons produced in coincidence with the ^{9}Li.

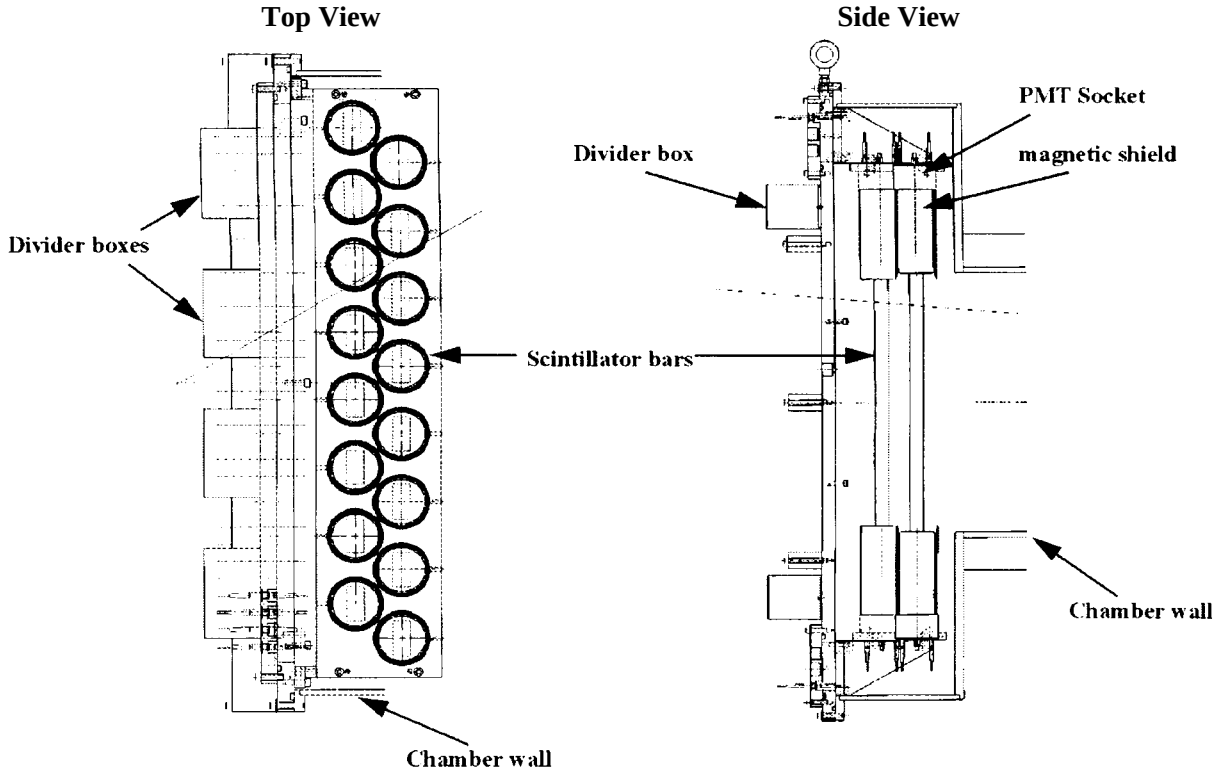

Figure 2 -- CAD drawings of the plastic scintillator array at the exit of the Beam- Sweeping Dipole. Particles are incident on the array from the right.

The surfaces of the scintillator bars have no reflecting material added, so that all scintillation light created within a cone of critical angle with respect to the scintillator surfaces is transmitted to the ends of the

bars by total internal reflection. A memory of the vertical position of the fragment is thus retained. The mean of the two signals gives a pulse height which is independent of the position of the source of the light.

The PMTs are biased and read out by high voltage bases built at the NSCL. The bases are modified versions of the Hamamatsu model E394 base. The first modification to the Hamamatsu design is that the resistors in the NSCL version have half the resistance of the Hamamatsu version. This doubles the bleeder current through the device, helping to retain linearity for large pulses. The second modification is that the bases are split into two separate modules. Inside the vacuum chamber a socket device containing the capacitive portion of the circuit is connected directly to the PMTs. These sockets are connected via ribbon cable feed-throughs to the resistor chains on the outside of the vacuum chamber. The voltage dividers are placed outside the vacuum to dissipate heat generated in the resistors, preventing both gain drifts from resistive heating and damage to the system from excessive heating of the bases. Two signals are pulled from each phototube base. In addition to the anode pulse, which is integrated by a charge-to-digital converter for an energy measurement, a signal from the eleventh of the twelve dynodes is inverted and used for timing purposes.

To monitor what gain drifts do occur, a blue light-emitting diode is fixed to the face of each PMT. The LEDs are fired at a rate of one pulse per second throughout the experiment, and the resulting PMT signals are recorded along with the experimental data. Offline analysis showed that over the course of a several-week experiment the gain drifts of the PMTs were negligible compared to the resolution of the scintillator array.

A stainless steel vacuum chamber contains the detectors and couples the system to the beamline. In the beamline is a pair of gas-filled PPACs used to measure the incoming beam particles' directions. The far upstream end of the vacuum chamber is coupled to the beamline through a gate valve which can be closed to isolate the chamber from the beamline, allowing rapid pump down and venting of the chamber while the PPACs stay in the vacuum of the beamline. Between the gate valve and the magnet are vertical lengths of pipe extending above and below the chamber. A large target ladder, capable of holding 7 reaction targets 5.1 cm high and 7.6 cm wide is mounted in the pipe. The target ladder is manipulated by a push rod that can be run up or down by hand to change the target.

Between the coils of the magnet, 15.2 cm downstream from the target ladder, are located the Si strip detectors. The detectors are mounted on an aluminum rail that is bolted to an ISO flange on one side of the chamber. The flange includes feed-throughs for all cable connections to the detectors and can be quickly removed and replaced with a standard blank-off for work in the chamber that does not involve the silicons. A mounting rack for the Si preamps is clamped to the chamber to ensure a solid ground between the vacuum chamber and the preamp cases. When bolted into place, the preamps are suspended directly in front of the feed-through flange, allowing the cables between the preamps and the flange to be only a few cm long, minimizing their tendency to pick up noise.

The performance of Si detectors may be impaired by thermal noise. Our detectors are placed between the coils of a room temperature magnet that becomes considerably warmer than room temperature when operating. In test runs with the device, we found that as the magnet coils warmed the vacuum chamber, radiative heating of the silicons from the chamber walls quickly increased the leakage current of the detectors and impaired their resolution. To reduce such heating, a copper shroud was built and installed inside the chamber between the pole faces, shielding the detectors from the warm surfaces of the vacuum chamber. The shroud is a box with a rectangular opening for the beam particles to enter, and the entire downstream end is open for fragments to leave the detector over a large range of angles. The shroud is insulated from the vacuum chamber by ceramic feet, and copper lines are soldered onto its surface. Cold domestic water flows through the lines, cooling the shroud and shielding the Si detectors from the warm chamber walls. When the magnetic field is ramped up or down, eddy currents in the copper shroud tend to

pull it around the chamber. To fix it in place, two stainless steel studs were welded to the chamber, and the shroud was bolted down.

The purpose of the magnet is to prevent neutrons produced in the fragment detectors from reaching the Neutron Walls. Sweeping the beam is not alone enough to ensure that no neutrons from the detectors will reach the Walls. Using the maps of the magnetic fields, the trajectories of unreacted beam particles are calculated through the magnet to determine where they strike the scintillator array. Outside the vacuum chamber, directly behind the plastic array, a stack of brass and steel shielding is assembled to absorb detector neutrons as they exit the chamber. The thickness of the stack has been 30 - 60 cm. In addition, brass bars 5 cm thick are bolted to the inside of the aluminum detector plate a few cm behind the scintillators. The shielding essentially eliminates fragment-1n coincidences resulting from reactions in the plastic array.

The scintillator array is calibrated by using the NSCL A1200 Spectrograph to create a beam of fragments of the type that will be measured in the experiment. The field of the dipole magnet is adjusted to sweep the beam over the scintillator array, illuminating as many bars as the bending power of the magnet permits. The pulse height of scintillation light produced in the plastic bars is not directly proportional to the amount of energy deposited in the detector by the fragment. For our purposes, an acceptable parameterization of the light production is achieved by the method developed by D. Cebra, *et al.* [9]. All detectors are gain matched, and then the pulse height is converted into light intensity in units of MeV electron equivalent (MeVee) by the equation:

$$L=0.265(E^{1.39}/Z^{0.78}A^{0.41})$$

where E is the total energy of the fragment in MeV, and Z and A are the atomic and mass numbers of the fragment. A linear relation was thus obtained between measured pulse height and L. For ^{9}Li particles of 25 MeV/A, an energy resolution of 1.4%, FWHM was achieved.

Isotopic identification of charged fragments and beam particles is achieved by the ΔE-E method. For each particle, the energy loss measured by the Si detectors is plotted against the total energy measured by the silicon and the plastic bars. Figure 3a is a ΔE-E plot measured between the Si strips and the scintillator array in a ^{11}Li experiment.

The ΔE-E spectra from bars which stopped the ^{11}Li beam show some contamination between the ^{9}Li and ^{11}Li regions of the plots. This contamination is caused by ^{11}Li particles which lost some of their energy in the detector before dissociating and liberating two neutrons. The neutrons then carried off energy not detected by the scintillator, yielding a lower than normal energy measurement for that particle. However, shielding blocks behind the scintillator bars prevented these neutrons from reaching the neutron detectors, and the set of ^{9}Li-2n coincidence events shows no such contamination. A plot of ΔE-E for ^{9}Li-2n coincidences is shown in Figure 3b, and the ^{9}Li region is more sharply defined.

To perform a TOF measurement of neutrons detected in the Neutron Walls, the fragment detection system must also provide a time signal when the fragment leaves the target. Ideally, this signal would come from the silicon strip detectors, as the 15-cm flight path between target and detector would require a negligible correction for the fragment's flight time. However, in the vicinity of the dipole magnet power supplies, the fast outputs of the silicon pre-amps are prone to noise-pickup problems, and the system is unstable. A more reliable time signal is obtained from the dynode signals of the plastic array PMTs. To compensate for the varying transit times of light from different source points in a scintillator bar, the average of the time signals from each bar's two PMTs is calculated. The inherent timing resolution of the scintillator bar-Neutron Wall combination is illustrated by events in which the primary beam reacts in the plastic of the fragment array, creating γ rays which are detected by the Neutron Walls. A TOF spectrum for γ rays created by an ^{18}O beam in the bars is shown in Fig. 4. There are six channels per nanosecond, and the resolution of the γ-ray peak is 0.8 ns, FWHM.

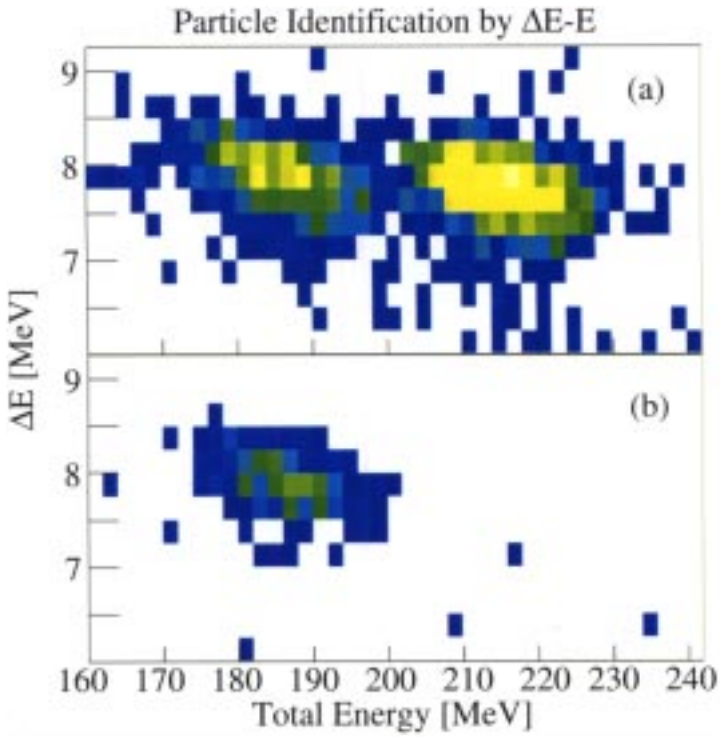

Figure 3 -- ΔE-E plots from ^{11}Li experiment. Only the region around ^{11}Li and ^{9}Li is shown. a) ^{9}Li and ^{11}Li for all event types, including fragment singles as well as fragment-1n and fragment-2n coincidences. b) Particle identification plot for fragment – 2n coincidences only.

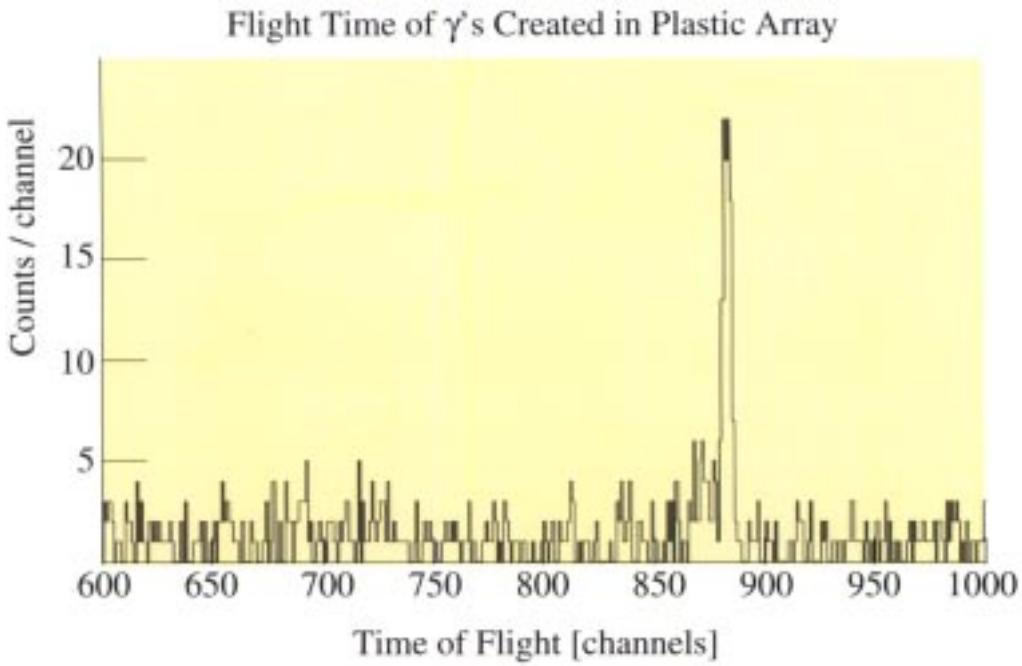

Figure 4 -- TOF of γ-rays created in scintillator bars by a beam of ^{18}O and detected by the Neutron Walls. The peak has a resolution of 0.8 ns, FWHM.

To find the absolute zero of the time calibration, that is, to get around the effect of varying PMT transit times and cable lengths, a ^{60}Co γ-ray source is used. The source is positioned inside the vacuum chamber near the Si detectors, and γ–γ coincidences are recorded between the 16 scintillator bars and the 48 cells of the Neutron Walls. Because of the small pulse height of these events, the time resolution of the ^{60}Co coincidence spectrum is inferior to the spectrum from beam-induced γ rays produced in the scintillators. However, a long acquisition time with the source provides excellent statistics, and even with a resolution of 3.5 ns, FWHM, these data provide adequate time calibration for bars which stopped low numbers of beam particles, and show no beam-induced γ–ray peak.

When measuring the TOF of neutrons and γ rays created in the target, a correction is made for the flight times of the fragments traveling from the target to the bars, because the time signal from the bars is used as the neutron TOF stop. For ^{9}Li fragments varying in energy from 20 to 30 MeV/A and in angle into the magnet from –10° to +10°, the flight paths from the target to the front of the plastic array differ by less than 2 cm, corresponding to 0.3 ns. An additional 4.75 cm of flight path length is added for events in which the fragment is detected by bars in the second row of the staggered array (see Fig. 2.) After a fragment's energy is determined from the size of the light pulse, its velocity and TOF from target to detector are calculated, and that time is added to the neutron TOF measurement for each event.

The status of each experiment done with the fragment detection system is listed below.

1. "Evidence for an *l*=0 Ground State in ^{9}He," L.Chen, B. Blank, B.A. Brown, M. Chartier, A. Galonsky, P.G. Hansen and M. Thoennessen, Phys. Rev. Lett., submitted.
2. "Dissociation of ^{8}He," Y.Iwata, K. Ieki, A. Galonsky, J.J. Kruse, J. Wang, P.D. Zecher, F.Deak, A. Horvath, A. Kiss, Z. Seres, J.J. Kolata, J. von Schwartzenberg, R.E. Warner and H. Schelin, Phys. Rev. C, submitted.
3. "Identification of the ^{10}Li Ground State," M. Chartier, J.R. Beene, B. Blank, L. Chen, A. Galonsky, N. Gan, K. Govaert, P.G. Hansen, J. Kruse, V. Maddalena, M. Thoennessen and R.L. Varner, Phys. Lett. B, submitted.
4. "Final-State Interactions in the N=7 Systems (^{8}He+n) and (^{9}Li+n)," L.Chen, T. Aumann, B. Blank,B.A. Brown, M. Chartier, F. Deak, A. Galonsky, P.G. Hansen, A. Horvath , K. Ieki, Y. Iwata, Y. Higurashi, , A. Kiss, J. Kruse, V. Maddalena, Z. Seres , S. Takeuchi and M. Thoennessen, Phys. Rev.Lett., in preparation.
5. "The Coulomb Excitation of ^{6}He," J. Wang, A. Galonsky, J. Kruse, D. Morrissey, M. Steiner, E. Tryggestad, R.White-Stevens, P. Zecher, F. Deak, A. Horvath, A. Kiss, Z. Seres, Y. Ando, K. Ieki, Y. Iwata, J.J. Kolata, J. Schwarzenberg and R.E. Warner, Phys. Rev. C, in preparation.
6. "The Coulomb Excitation of ^{11}Li," J.J. Kruse, A. Galonsky, D. Morrissey, M. Steiner, E. Tryggestad, J. Wang, R.White-Stevens, P. Zecher, F. Deak, A. Horvath, A. Kiss, Z. Seres, Y. Ando, K. Ieki, Y. Iwata, J.J. Kolata, J. Schwarzenberg and R.E. Warner, Phys. Rev. C, in preparation.
7. "A Measurement of the ^{14}C(n,γ)^{15}C Cross Section at Astrophysical Energies by Inverse Kinematics," J. Weiner,. A. Galonsky, K. Ieki, Y. Iwata, Y. Higurashi, F. Deak, A. Horvath, A. Kiss, Z. Seres, J.J. Kolata, J. von Schwartzenberg and H. Schelin, Astrophysical Journal, in preparation.
8. "Cross Section for the ^{8}Li(n,γ)^{9}Li Reaction at Astrophysical Energies," H. Kobayashi, Y. Higurashi, K. Ieki, Y. Iwata, A. Galonsky, F.Deak, A. Horvath, A. Kiss, Z. Seres, J.J. Kolata and H. Schelin, Astrophysical Journal, in preparation.
9. "S_{17}(0) Determined from the Coulomb Breakup of 83 MeV/nucleon ^{8}B," B. Davids, D.W. Anthony, Sam M. Austin, T. Baumann, D. Bazin, R.R.C. Clement, C.N. Davids, H. Esbensen, P.A. Lofy, T. Nakamura, B.M. Sherrill, J.A. Tostevin and J. Yurkon, Phys. Rev. Lett., in preparation.

We acknowledge Dr. Rich Tighe for his help in securing the dipole magnet from Lawrence Berkeley Laboratory, and we thank Jim Vincent for the construction of the PMT bases and divider chains. We are also

indebted to Doug Harris, Jon Brandon and Harold Hilbert for help with construction and installation of the magnet system.

a. Department of Physics, Rikkyo University, 3-Nishi-Ikebukuro, Toshima, Tokyo 171, Japan

[1]Present address: Mayo Clinic Dep't. of Radiation Oncology, 200 1st St. SW, Rochester, MN 55905, USA
[2]Present address: American Express Co., 3WFC,4712B, 200 Vesey St., New York, NY 10285, USA
[3]Present address: NIRS, 4-9-1 Anagawa, Inage, Chiba 263-8555, Japan
[4]Present address: Investor Analytics LLC, 80 Broad Street, New York, NY 10004, USA

References

1. R. Anne, S.E.Arnell, R. Bimbot, H. Emling, D. Guillemaud-Mueller, P.G. Hansen, L. Johannsen, B. Jonson, M. Lewitowicz, S. Mattson, A.C. Mueller, R. Neugart, G. Nyman, F. Pougeon, A. Richter, K. Riisager, M.G. Saint-Laurent, G. Schrieder, O. Sorlin, and K. Wilhelmsen, Phys. Lett. B 250 (1990) 19.
2. D. Sackett, K. Ieki, A. Galonsky, C.A. Bertulani, J.J. Kruse, W.G. Lynch, D.J. Morrissey, N.A. Orr, H. Schulz, B.M. Sherrill. A. Sustich, J.A. Winger, F. Deak, A. Horvath, A. Kiss, Z. Seres, J.J. Kolata, R.E. Warner, and D.L. Humphrey, Phys. Rev. C 48 (1993) 118.
3. K. Ieki, D. Sackett, A. Galonsky, C.A. Bertulani, J.J. Kruse, W.G. Lynch, D.J. Morrissey, N.A. Orr, H. Schulz, B.M. Sherrill. A. Sustich, J.A. Winger, F. Deak, A. Horvath, A. Kiss, Z. Seres, J.J. Kolata, R.E. Warner, and D.L. Humphrey, Phys. Rev. Lett. 70 (1993) 730.
4. D. Sackett Ph.D. Thesis, Michigan State University (1992)
5. D. Swan, J. Yurkon, D.J. Morrissey, Nucl. Instr. & Meth. A348, (1994) 314.
6. P.D. Zecher, A. Galonsky, J.J. Kruse, S.J. Gaff, J. Ottarson, J. Wang, F. Deak, A. Horvath, A. Kiss, Z. Seres, K. Ieki, Y. Iwata and H.R. Schelin, Nucl. Instr. & Meth. A401 (1997) 329.
7. B. Davin et al., Nuclear Instruments and Methods in Physics Research, to be submitted.
8. D. Cebra, W.K. Wilson, A. Vander Molen and G.D.Westfall, Nucl. Instr. & Meth. **A313** (1992) 367.